

TABLE II. Final states corresponding to irreducible representations of D_{3h} .^a

A_2'	$RRR+LLL$	$RRL+LRR+RLR+LLR+RLL+LRL$
A_2''	$RRR+LLL$	$RRL+LRR+RLR+LLR+RLL+LRL$
E'	$(2 RRL-LRR-RLR-2 LLR+RLL+LRL, 2 RRL-RRL-LRR-2 LRL+LLR+RLL)$	
E''	$(2 RRL-LRR-RLR+2 LLR-RLL-LRL, 2 RRL-RRL-LRR+2 LRL-LLR-RLL)$	

^a The irreducible representations A_2' , A_2'' , E' and E'' , of D_{3h} can be identified by their characters for E , C_3 , σ_h , and σ_v :

A_2'	1	1	1	-1
A_2''	1	1	-1	1
E'	2	-1	2	0
E''	2	-1	-2	0

Table I describes the basic step of the process and so fixes the conventions adopted; Table II lists the results.

The selection rules are obtained by requiring that the initial and final states have the same transformation properties under D_{3h} . One finds immediately that, for the case being considered, annihilation into three photons is forbidden for scalar (or pseudoscalar) particles: less symmetrical annihilations into three photons, however, are not forbidden for scalar (or pseudoscalar) particles on the ground of rotational symmetry³ but ordinarily are forbidden by invariance under charge conjugation.⁶ For vector and pseudovector particles we consider the polarized states using the normal to the plane of the photons as the axis of quantization. The vector state with $m=0$ can decay only into A_2'' final states, while the corresponding pseudovector state must decay into A_2' states. The only final states allowed for a vector (pseudovector) state with $m=\pm 1$ are the states $E'(E'')$.

These considerations are of interest in connection with experiments⁷ on the three-photon annihilation of the 3S state of positronium, a vector state. This encourages a study of some observable properties of the final states A_2'' and E' by expanding them in plane-polarized components. The results are given in Table III, where those for E' correspond to a statistical mixture

TABLE III. Polarization probabilities for the A_2'' and E' states.^a

A_2''	$RRR+LRR+RLR+LLR+RLL+LRL$	$P(\perp) = \frac{5}{1}$	$P'(\perp) = \frac{9}{1}$
E'	$(2 RRL-LRR-RLR-2 LLR+RLL+LRL, 2 RRL-RRL-LRR-2 LRL+LLR+RLL)$	$P(\perp) = \frac{2}{1}$	$P'(\perp) = \frac{1}{1}$

^a $P(\perp)$ [or $P(\parallel)$] is the probability that one photon be observed polarized perpendicular to the plane of the photons (or in the plane). $P'(\perp)$ [or $P'(\parallel)$] is the probability that when one photon is observed polarized normal to the plane, one of the other two be observed polarized normal to the plane (or in the plane).

of the initial states with $m=1$ and $m=-1$, and agree with results of a perturbation calculation by Drisko.⁸ The A_2'' state, $RRR+LLL$, has not been considered since it does not occur in the lowest order perturbation calculation; however, we have found no fundamental reason for excluding it. It should also be noted that to predict the results of experiments with the unpolarized vector state, it is necessary to know the ratio of the symmetrical decay cross section for $m=0$ and $m=\pm 1$ states, and this cannot be determined from invariance arguments such as we have given.

It is a pleasure to thank Mr. R. Drisko for discussing his results with us and letting us quote them prior to publication and to thank Professor H. C. Corben, Fulbright Visiting Professor at the University of Milan, for useful discussions.

^a A preliminary report on this work was presented by one of us (F.G.F.) to the Seminario Matematico e Fisico di Milano on January 28, 1952. The work was completed during the stay of F. G. F. at Carnegie Institute of Technology in 1952.

¹ L. Landau, Doklady Akad. Nauk. S.S.S.R. **60**, 207 (1948).

² C. N. Yang, Phys. Rev. **77**, 242 (1950).

³ D. C. Peaslee, Helv. Phys. Acta **23**, 845 (1950).

⁴ L. Michel, Compt. rend. **234**, 703 (1952); **234**, 2161 (1952).

⁵ The notation is the same as that of J. E. Rosenthal and G. M. Murphy, Revs. Modern Phys. **8**, 317 (1936).

⁶ L. Wolfenstein and D. G. Ravenhall, Phys. Rev. **88**, 279 (1952).

⁷ S. DeBenedetti and R. Siegel, Phys. Rev. **85**, 371 (1952).

⁸ R. Drisko, private communication.

Secondary Particles Resulting from 375-Mev Alpha-Bombardment of Nuclei

R. W. DEUTSCH

Radiation Laboratory, Department of Physics, University of California, Berkeley, California

(Received March 11, 1953)

A PROGRAM¹ has been undertaken to analyze the secondary particles which result from high energy bombardment of nuclei. In the present experiment, thin targets of Be, Al, Ni, Ag, Au, and U have been bombarded by 375-Mev alpha-particles of the 184-inch cyclotron. Secondary particles then spiral down into Ilford C2, 200 μ nuclear track plates which are located at three positions below the median plane of the cyclotron. The description of the apparatus can be found in reference 1. The analysis of the secondary particles is similar to that found in reference 1.

Table I shows the secondary particles with which we are concerned and their mean energies in each position.

Table II shows the results obtained. Each element is normalized to 100 percent for the number of particles found per unit solid angle per unit radius of curvature interval.

The hydrogen and helium isotopes are identified individually. For the heavier isotopes, only Li⁸ and B⁸ could be resolved in each position. They are recognizable because of the characteristic hammer at the end of the range. Li⁷ could be identified only in the 42-46 cm position. Li⁶ and Be⁷ form a common locus which is separable in each position although there is possible contamination by carbon isotopes in the 21-24.5 cm position. For the remaining heavy secondary particles, there was overlapping

TABLE I. Mean energies of secondary particles in Mev. The target thickness in mg/cm² for each element was the following: Be (8.67), Al (1.67), Ni (8.10), Ag (12.8), Au (11.7), U (23.0). No correction for target thickness has been made. It is significant for particles of short range.

Radius of curvature interval	42-46 cm	29-32.5 cm	21-24.5 cm
H ¹	18.5	9.1	5.0
H ²	9.3	4.6	2.5
H ³	6.2	3.0	1.7
He ³	24.9	12.2	6.6
He ⁴	18.8	9.2	5.0
He ⁶	12.5	6.1	3.3
He ⁷	10.7	5.2	2.9
Li ⁶	28.2	13.8	7.5
Li ⁷	24.2	11.8	6.4
Li ⁸	21.2	10.3	5.6
Li ⁹	18.8	9.2	5.0
Be ⁷	43.0	21.0	11.4
Be ⁹	33.0	16.3	8.9
Be ¹⁰	30.1	14.7	8.0
B ⁸	58.8	28.7	15.6
B ¹⁰	47.0	22.9	12.5
B ¹¹	42.7	20.8	11.3
B ¹²	39.2	19.1	10.4
C ¹⁰	67.7	33.0	18.0
C ¹¹	61.5	30.0	16.3
C ¹²	56.4	27.5	15.0
C ¹³	52.1	25.4	13.9
C ¹⁴	48.3	23.7	12.9

TABLE II. Abundance distribution of products. Each element has been normalized to 100 percent for the number of particles found per unit solid angle per unit radius of curvature interval. The actual number of tracks found are in brackets and are listed below the percentages in each case.

Radius of curvature interval	42-46 cm						29-32.5 cm						21-24.5 cm					
	Be	Al	Ni	Ag	Au	U	Be	Al	Ni	Ag	Au	U	Be	Al	Ni	Ag	Au	U
H ¹	10.92 (163)	12.10 (199)	13.36 (239)	17.37 (194)	29.62 (178)	28.74 (204)	8.36 (119)	13.57 (214)	26.88 (401)	38.56 (499)	19.59 (402)	9.79 (271)	6.50 (125)	14.82 (276)	31.16 (491)	15.90 (508)	1.67 (196)	2.45 (137)
H ²	3.62 (54)	2.43 (40)	2.63 (47)	3.40 (38)	3.16 (19)	2.26 (16)	3.94 (56)	1.97 (31)	0.87 (13)	0.15 (2)	0.09 (2)	0.33 (9)	2.08 (40)	0.65 (12)	0.19 (3)	0.06 (2)	0.14 (16)	0.25 (14)
H ³	2.75 (41)	0.48 (8)	0.34 (6)	0.09 (1)	0.17 (1)	0.42 (3)	2.32 (33)	0.19 (3)	0.34 (5)	0.15 (2)	0.09 (2)	0.25 (7)	1.51 (29)	0.43 (8)		0.03 (1)	0.08 (9)	0.15 (8)
He ³	2.68 (40)	1.46 (24)	1.29 (23)	1.07 (12)	1.16 (7)	1.13 (8)	4.29 (61)	1.33 (21)	1.01 (15)	0.08 (1)	0.15 (3)	0.47 (13)	2.76 (53)	0.59 (11)	0.38 (6)	0.06 (2)	0.17 (20)	0.27 (15)
He ⁴	10.52 (157)	9.67 (159)	7.88 (141)	17.46 (195)	28.29 (170)	18.60 (132)	19.19 (273)	14.97 (236)	8.51 (127)	2.24 (29)	1.17 (24)	3.87 (107)	12.59 (242)	11.70 (218)	2.22 (35)	0.25 (8)	0.49 (58)	4.01 (224)
Li ⁶ , Be ⁷	0.74 (11)	0.42 (7)	0.50 (9)	0.63 (7)	1.50 (9)	1.55 (11)	0.63 (9)	1.14 (18)	0.47 (7)		0.34 (7)	0.47 (13)	0.83 (16)	0.48 (9)	0.19 (3)		0.43 (5)	0.38 (21)
Li ⁷	0.33 (5)	0.48 (8)	0.34 (6)	0.27 (3)	0.83 (5)	0.28 (1)												
Li ⁸	0.07 (1)						0.28 (4)						0.16 (3)					0.02 (1)
B ⁸	0.07 (1)	0.06 (1)												0.05 (1)				
I	0.27 (4)	0.42 (7)	0.06 (1)	0.27 (3)	0.17 (1)		0.77 (11)	1.46 (23)	0.47 (7)	0.38 (5)	0.68 (14)	0.43 (12)						
II	0.07 (1)	0.18 (3)	0.06 (1)	0.09 (1)	0.17 (1)	0.42 (3)	0.21 (3)	1.27 (20)	0.14 (2)	0.08 (1)	0.09 (2)	0.32 (9)						
III		0.12 (2)	0.06 (1)	0.18 (2)	0.71 (5)													
Not classified	0.13 (2)	0.61 (10)	0.22 (4)	0.81 (9)	8.15 (49)	16.91 (120)	0.07 (1)	3.30 (52)	0.14 (2)	0.23 (3)	1.27 (26)	4.05 (112)	1.35 (26)	3.60 (67)	0.32 (5)	0.18 (6)	0.31 (37)	1.36 (76)

I—He⁶, Be⁹, B¹⁰, C¹¹
 II—Be¹⁰, B¹¹, C¹², C¹³
 III—He⁷, Li⁹, B¹², C¹⁴
 I—He⁶, Li⁷, Be⁹, Be¹⁰, B¹⁰, B¹¹, C¹¹, C¹², C¹³
 II—He⁷, Li⁹, B¹², C¹⁴

of ranges so that separation could only be made by groups in the 42-46 cm position and the 29-32.5 cm position. Carbon was the highest atomic number considered because the range-energy relations have not been verified for higher atomic number. However, higher atomic number could possibly fall into groups II and III in the 42-46 cm position and into groups I and II in the 29-32.5 cm position.

The minimum range accepted was 9 microns. All tracks that had a range greater than 9 microns but still too short to fall on a calculated locus were put in the "not classified" group. The resolution for the separation of the heavy isotopes decreases with energy so that in the 21-24.5 cm position only Li⁶ and Be⁷ could be separated, while all the rest fall into the "not classified" position. The 9-micron criterion eliminated very little information for the light elements, but for Au and U there were many tracks that were shorter. These doubtless included fission fragments.

The analysis of the results of this experiment are still in a preliminary stage. Similar experiments are being done with the same targets, but high energy protons and deuterons are being used as the bombarding particles. An angular distribution measurement using high energy alphas is also being made in order to separate the instantaneous emission of particles from the struck nucleus from the slow boiling off process.

The results of this experiment and reference 1 indicate that fragments of $A > 4$ are emitted from nuclei with high momenta. Dr. L. Alvarez has suggested as a possible mechanism that these heavy fragments are not created in the initial bombardment but are subsequently formed by the fission of resultant nuclei left in excited states.

I am particularly indebted to Dr. W. Barkas for his aid in guiding this entire program. I wish to thank Esther Jacobson for having scanned most of the plates.

¹ W. Barkas and H. Tyren, Phys. Rev. **89**, 1 (1953).

Dysprosium 157

THOMAS H. HANDLEY AND ELMER L. OLSON
Oak Ridge National Laboratory, Oak Ridge, Tennessee
(Received March 18, 1953)

AN 8.2 ± 0.1 -hour activity has been obtained by bombarding highly purified terbium oxide with 24-Mev protons in the ORNL 86-inch cyclotron.¹ Separations were made by ion ex-

change² and two radioactive species were found with the dysprosium fraction. There was an 8.2 ± 0.1 -hour activity from the $(p, 3n)$ reaction and a 134-day activity from the (p, n) reaction on Tb¹⁵⁹. The 134-day activity is Dy¹⁵⁹, as previously reported,³ and decays by pure electron capture.

A rough excitation function was run to aid in establishing the reaction and mass assignment for the 8.2-hour activity. This was done by wrapping a number of 5-mg samples of Tb₂O₃ in thin aluminum foil and making a stack of these with aluminum absorbers interspaced to adjust the proton energy. The method proved to be sufficient to differentiate between (p, n) , $(p, 2n)$, and

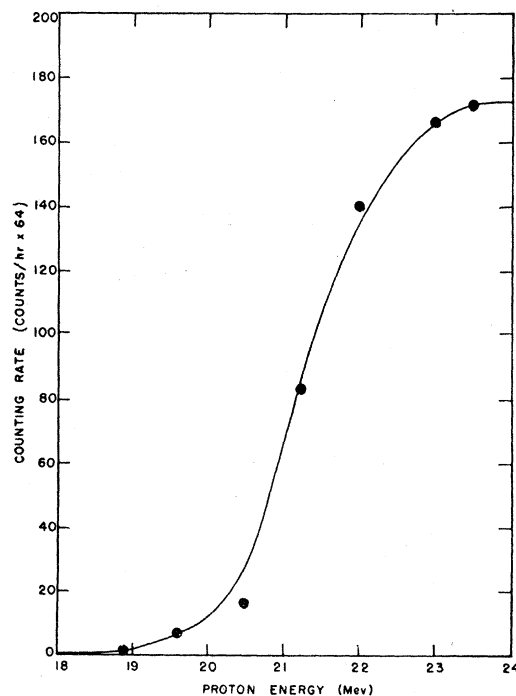


FIG. 1. Excitation function.